

Theoretical aspects of the luminescence of porous silicon

C. Delerue, G. Allan, and M. Lannoo

*Institut d'Electronique et de Microelectronique du Nord, Département Institut Supérieur d'Electronique du Nord,
41 Boulevard Vauban, 59046 Lille Cedex, France*

(Received 25 March 1993)

The luminescence in the visible range of porous silicon is analyzed in the hypothesis of quantum confinement. We calculate the electronic and optical properties of silicon crystallites and wires with sizes between 0 and 4.5 nm. The band-gap energies of such confined systems are in agreement with the photon energies observed in luminescence. We calculate the radiative recombination times of the confined excitons. We conclude that experimental nonradiative processes in porous silicon are more efficient than calculated radiative ones at $T=300$ K. The high photoluminescence efficiency of porous silicon is due to the small probability of finding a nonradiative recombination center in silicon nanocrystallites. Recently, it has been proposed that the low-temperature dependence of the experimental radiative decay time of the luminescence of porous silicon could be explained by the exchange splitting in the fundamental exciton. We show that the influence of the valley-orbit splitting cannot be excluded. The sharp optical-absorption edge above 3.0 eV is not proof of the molecular origin of the properties of porous silicon because silicon nanostructures present a similar absorption spectrum. We calculate the nonradiative capture of electrons or holes on silicon dangling bonds and show that it is very dependent on the confinement. We find that the presence of one dangling bond at the surface of a crystallite in porous silicon must destroy its luminescent properties above 1.1 eV but can produce a luminescence below 1.1 eV due to a radiative capture on the dangling bond.

PACS number(s): 73.20.Dx, 78.55.Hx

I. INTRODUCTION

The observation of intense photoluminescence from porous silicon¹ has stimulated considerable activity. Because of the large blueshift of the observed radiations with respect to the bulk silicon band-gap energy, it has been proposed that the quantum confinement in crystallites^{2,3} or wires^{1,4} is at the origin of the luminescence in the visible range. But this hypothesis has been challenged by models involving siloxene derivatives,⁵ polysilanes, or hydrides^{6,7} on the surface of porous silicon. Another suggestion is that the dominant luminescent material is amorphous in nature.^{8,9} The quantum confinement interpretation of the luminescence of porous silicon is supported by the evolution of the luminescence intensity and peak position with anodic oxidation^{2,3} which could lead to a progressive reduction in nanostructure sizes. More recently, studies have shown that thermal oxidation gives a similar blueshift of the luminescence peak.^{10,11} The confinement model also seems to be consistent with structural characterizations.¹²⁻¹⁵ From a theoretical point of view, many papers have shown that confinement in wires¹⁶⁻¹⁸ or dots¹⁹⁻²¹ with typical sizes under 6 nm could explain the important blue shift of the luminescence compared to bulk silicon. Anyway, many points are still under debate. In particular, the lifetime of the luminescence is very long, in the range between milliseconds and microseconds,^{12,22} and the decay mechanism of the luminescence is unclear. The influence of defects, in particular surface defects, on the luminescence needs to be studied. Recently, it has been shown that the optical excitation spectrum of porous silicon samples has an important threshold above 3 eV.^{12,23} It has been con-

cluded that the quantum confinement model is not valid because the optical threshold should be in the 1.5-eV range as in luminescence. In this paper, we analyze the interpretation of quantum confinement from the results of theoretical calculations on silicon crystallites and wires. The electron-hole recombination processes in such confined silicon structures are investigated. We show that predicted optical properties of silicon crystallites are consistent with optical experimental data on porous silicon.

II. ELECTRONIC STRUCTURE OF SILICON DOTS AND WIRES

There are many experimental evidences that porous silicon is characterized by complex structures with nanometer sizes.^{12-15,24} It is thus reasonable to expect that quantum confinement could be the origin of its luminescence. It was supposed that porous silicon consists of silicon wires because the chemical dissolution widens the pores and, for high dissolution, pores merge isolating silicon columns.¹ From structural analysis clusters of crystalline silicon (quantum dots) were also proposed,^{13,14,25} but the crystalline character of such nanostructures is sometimes questioned.^{9,26} Other studies show that the morphology of luminescent porous silicon is more complex, consisting, for example, of a three-dimensional (3D) network of quantum segments in a noodlelike or wool-ball structure.²⁷ The quantum structure describing porous silicon may probably be intermediate between dots and wires consisting, for example, of a wire with a varying diameter.²⁴ Therefore we have performed calculations about dots and wires to understand the

confinement effects in porous silicon (some preliminary results were already published in Ref. 19).

The calculation of the electronic structure of silicon crystallites and wires is done using the linear combination of atomic orbitals (LCAO) technique. We choose crystallites and wires with, respectively, spherical and cylindrical shapes. We suppose that the nanostructures have the same lattice structure and the same interatomic distance than bulk silicon. Experiments²⁸ show that a small lattice relaxation occurs perpendicular to the surface but its amplitude is small ($\Delta a/a$ between 3.7×10^{-4} and 46×10^{-4}) so it has no incidence on the electronic structure of porous silicon. In the case of crystallites, this allows us to use symmetry operations of the T_d point group which considerably reduces the size of the calculations (see Ref. 20 in which the authors use a similar simplification). We are able to treat clusters containing up to 2059 atoms (cluster size = 4.3 nm). We suppose that all the dangling bonds are saturated with hydrogen atoms. For simplicity, we suppose that there is no hydrogen-hydrogen interactions. The hydrogen atoms are simply used to simulate the bonds at the surface of the cluster and sweep surface states out of the fundamental band gap. In our LCAO approach, the silicon atoms are represented by one s and three p atomic orbitals, and the hydrogen atoms by one s orbital. For each nanostructure, we write the Hamiltonian matrix H and the overlap matrix S in the basis of atomic orbitals. Then we solve the secular equation $(H - ES)\Psi = 0$ to obtain the one-electron energies E and wave functions Ψ . To build up H and S matrices, we use the empirical parameters of Ref. 29 which include the interactions and the overlaps up to the third neighbors. These have been fitted to the best pseudopotential band structure of bulk silicon. Compared to tight-binding methods, such a procedure gives not only a good description of the valence band but also of the conduction band. Spin orbit is not included as its contribution is small in the case of silicon.

Results for the band-gap energy of silicon crystallites and wires with respect to the diameter are plotted in Fig. 1. As expected, the highest confinement energy is obtained for the crystallites which correspond to the 0D system. We have reported results for cylindrical wires in 100, 110, and 111 directions. There is a strong anisotropy between directions, in particular for small diameters. The observed radiations of porous silicon are in the energy range between 1.4 and 2.2 eV.^{2,3} From Fig. 1, we see that this could be compatible with crystallites sizes between 2.5 and 4.5 nm. Similar results have been obtained by different groups¹⁹⁻²¹ and our results agree with other published band-gap energies.^{17-21,30-34} Small discrepancies between all theoretical results do not change the conclusion that confinement could be at the origin of porous silicon luminescence. Anyway, for quantum wires, a very large blueshift ($h\nu > 2.0$ eV) can only be obtained for very small diameter (< 2.3 nm). In that case the stability of such structure in the same crystallographic system than bulk silicon is not obvious.³⁵ For the crystallites, the band-gap energy follows approximately a $d^{-1.39}$ law where d is the diameter. The exponent 1.39 is different from 2 which would have been obtained using an

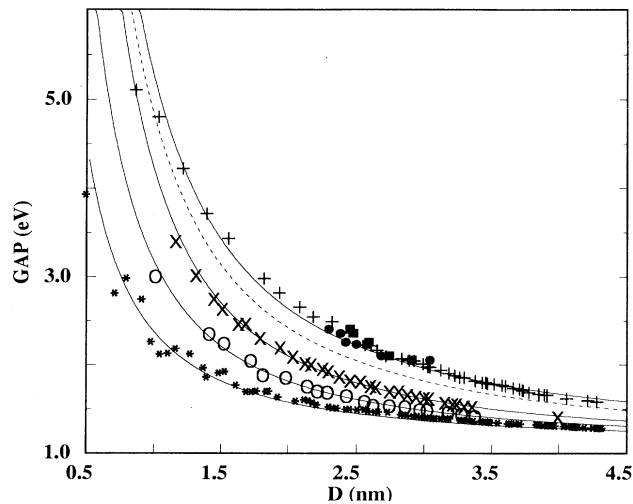


FIG. 1. Calculated optical band-gap energies for various silicon crystallites (+) or wires (100: ×; 110: *; 111: ○) with respect to their diameter d . The continuous lines are an interpolation and an extrapolation of these results by a d^{-n} law. The black dots and squares are the experimental results of Ref. 37. The dashed line is the band-gap energy for the crystallites including the Coulomb interaction between the electron and the hole.

effective-mass theory. It means that a good description of the bands is necessary. This is not surprising here in view of the large confinement energies. However, a careful analysis of our data shows that energies for large diameters tend to follow a law with a higher exponent which finally tends towards 2 at infinity when the effective-mass approximation becomes valid. Before comparing to experimental results, we include the Coulomb and correlation energies between the electron and the hole which has been estimated in Ref. 36 for spherical crystallites. The dashed line in Fig. 1 represents the variation of the electron-hole pair energy with respect to the diameter of the crystallites. The correlation energy is negligible in the range of interest here and the attractive Coulomb energy³⁶ between the electron and hole is approximated by $-3.572(e^2/\epsilon d)$. We also report in Fig. 1 experimental results³⁷ on optical band gaps measured on small hydrogenated silicon crystallites. Two sets of results are plotted (black dots and squares), differing by the method to evaluate the size of the crystallites. The agreement between theory and experiment is good, taking into account the uncertainties. This represents a positive test of our calculation and supports a posteriori the fact that the silicon particles have a crystalline character.³⁷ Finally, we find that the confinement energy is slightly more important for valence states than for conduction states.¹⁶ This depends of the crystallite size and for increasing radii, 65–55% of the total confinement energy is in the valence band.

III. LUMINESCENCE OF SILICON NANOSTRUCTURES

In the hypothesis of quantum confinement, the luminescence of porous silicon is expected to be due to

the radiative recombination of electron-hole pairs from the lowest exciton states whose binding energies are enhanced compared to bulk silicon. If the widening of the gap is an obvious consequence of the confinement, it is more difficult to predict its influence on the efficiency of radiative processes compared to nonradiative ones. In bulk silicon, because of its indirect band gap, the emission of light is only possible with the assistance of phonons to supply momentum in a second-order process.³⁸ Therefore the luminescence of bulk silicon is weak as nonradiative recombinations become more efficient. The confinement of the electron-hole pair in real space leads to a spread of the wave functions in the reciprocal space and then radiative recombination can occur in a first-order process.³⁸ In this part we try to estimate the evolution of the first-order radiative recombination probability with respect to the confinement. We also look at its variation with the temperature. Some preliminary results were already published.³⁹

The radiative recombination time τ of a first-order radiative process is defined from the Fermi golden rule and is given by⁴⁰

$$\frac{1}{\tau} = \frac{16\pi^2}{3} n \frac{e^2}{h^2 m^2 c^3} E_0 |\langle i_{BC} | p | f_{BV} \rangle|^2, \quad (1)$$

where $|i_{BC}\rangle$ is the initial state of the electron in the conduction band and $|f_{BV}\rangle$ is the final state in the valence band (i.e., the hole state). E_0 is the energy of the transition and n is the refractive index of porous silicon. From ellipsometry⁴¹ and optical-absorption⁴² experiments, it seems that the refractive index decreases with increasing porosity. We choose a value of 1.33 which has been given for porous layer with a porosity of 74%.⁴² The momentum matrix element $|\langle i_{BC} | p | f_{BV} \rangle|^2$ is developed in the tight-binding basis. In the case of crystallites, Eq. (1) takes into account the 3D confinement of the exciton. In effect, as the crystallite radius is smaller than the silicon free-exciton Bohr radius (~ 43 Å), the wave function of the exciton is well approximated by the product $|i_{BC}\rangle |f_{BV}\rangle$. In the case of wires, we should multiply Eq. (1) by an excitonic factor which is assumed to be close to one.³⁰ The calculation is done replacing the atomic orbitals by Gaussians.⁴³ Note that this procedure has been used to predict the optical cross section of the isolated dangling bond in silicon.⁴⁴ The calculation of the recombination rate of Eq. (1) corresponds to a one-electron theory: the spin is not included and therefore the effects due to the exchange interactions are neglected. As discussed below, the exchange splitting must have an important effect on the low temperature dependence of the radiative recombination rate.⁴⁵

Measurements of the dependence of photoluminescence decay rates on photon energy were made at room temperature. Therefore we have included the effect of the temperature for a best comparison. To do that, we calculate the probability $W_{n,n'}$ of optical transition between two states n and n' , respectively, of the conduction and valence bands [Eq. (1)]. The thermally averaged recombination rate is given by

$$\left\langle \frac{1}{\tau} \right\rangle = \frac{\sum_{n,n'} W_{n,n'} \exp\left[-\frac{E_{n,n'}}{kT}\right]}{\sum_{n,n'} \exp\left[-\frac{E_{n,n'}}{kT}\right]}, \quad (2)$$

where $E_{n,n'}$ is the photon energy of the transition, k is the Boltzmann constant, and T is the temperature [the spin degeneracy is not included in the sum of Eq. (2): its inclusion would divide the recombination rate by a factor 2 as only transitions between states with same spin are allowed]. This assumes that the thermalization of the electron and the hole after excitation in the bands is more efficient than the radiative recombination. We will see later that this is reasonable because the radiative recombination is not very efficient.

Figure 2 is a plot of the calculated recombination rate ($1/\tau$) for many spherical crystallites with different diameters. We present $1/\tau$ versus the calculated photon energy of each crystallite because information concerning the diameters is not available experimentally. Results of Fig. 2 correspond to the radiative recombination at $T=5$ K. The scattering of the calculated rates in Fig. 2 is very important. The first reason for this scattering is the fact that the symmetry representations of electron and hole states in the T_d point group can change very quickly from one crystallite to another and the optical matrix element is very sensitive to these changes (some transitions are even forbidden). For example, for big crystallites, there are six nearly degenerate states coming from the six equivalent minima of the conduction band. They give rise to one A_1 state, one twofold degenerate E state, and one threefold degenerate T_2 state whose splitting (valley-orbit splitting) between them is of the order of 10 meV

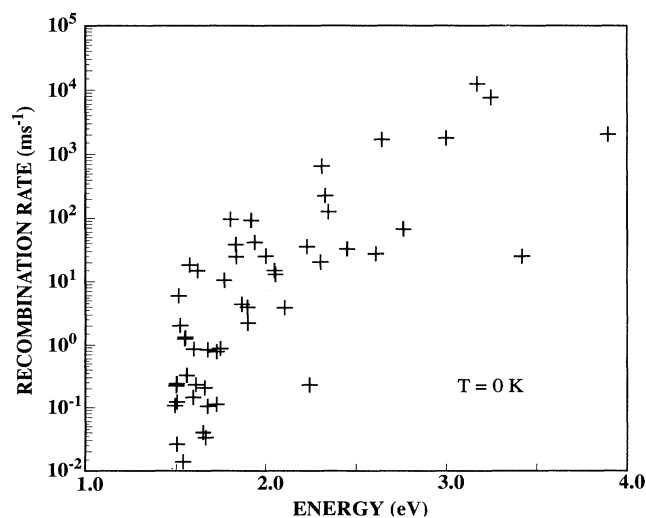


FIG. 2. Calculated recombination rate (ms^{-1}) of an excited electron-hole pair in silicon crystallites (crosses) with respect to the photon energy at 5 K. The spin degeneracy is not included: its inclusion would divide the calculated recombination rates by a factor of 2.

for the biggest crystallites that we have studied here. But the lowest state can be any one of the three depending on the size of the cluster. The second reason for this scattering is that the optical matrix element is proportional to the reciprocal space overlap of the electron and hole wave functions which is a strongly oscillating function of the size of the crystallites.³⁸ Note that this oscillation disappears in case of direct-gap materials.

There are some global features which can be extracted from results of Fig. 2. For crystallites with an optical gap larger than 2.3 eV (sizes lower than 2.5 nm), the radiative recombination is quite efficient with a characteristic time lower than 10 μ s. The mixing of different k states is important and the clusters get optical properties intermediate between an indirect-gap and direct-gap material.^{17,21} This result opens very interesting perspectives for further applications involving silicon crystallites. Another feature of Fig. 2 is the strong decrease of the radiative recombination rate for lower photon energy. This is obviously due to the indirect nature of the silicon band gap which gives a radiative recombination rate equal to zero in the limit of bulk silicon (in a first-order theory). The decrease is very abrupt for energies lower than 2 eV and then the radiative recombination becomes quite slow. A decrease of the decay rate of the luminescence for lower photon energy is also observed experimentally.^{12,22}

Figure 3 presents the calculated thermally averaged recombination rates for the same silicon crystallites as on Fig. 2 ($T = 5$ K) but for $T = 300$ K. Compared to Fig. 2, we see that the scattering of points is reduced. This is due to the averaging over the nearly degenerate states of different symmetry which cancel the effect of valley-orbit splitting previously described. Nevertheless, the scattering due to the oscillating nature of the k -space overlap of

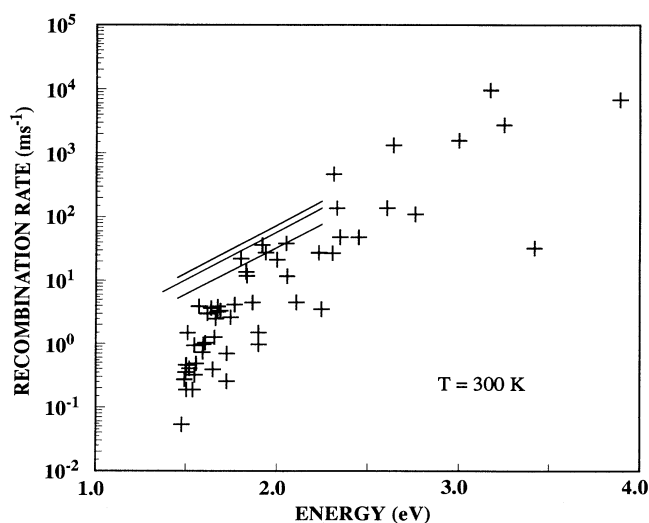


FIG. 3. Calculated recombination rate (ms^{-1}) of an excited electron-hole pair in silicon crystallites (crosses) with respect to the photon energy at 300 K. The spin degeneracy is not included: its inclusion would divide the calculated recombination rates by a factor of 2. Continuous lines plot the experimental dependence (Ref. 22) of decay rates on photon energy for three 65% porosity layers that differ by oxidation level.

the conduction and valence wave functions remains. In comparison to our theoretical results, we plot the dependence of photoluminescence decay rates given in Ref. 22. We see that, on average, the calculated radiative recombination rates are about one order of magnitude lower than the experimental decay rate.¹⁹ This is particularly true for photon energies lower than 2.0 eV. This means that, even if the confinement brings some momentum mixing to allow first-order optical transitions, the radiative recombination is probably less efficient than nonradiative processes at 300 K as concluded from some experimental studies.^{22,46} For a photon energy around 1.8 eV (typical luminescence peak energy of porous silicon), we predict an average radiative recombination time of about 1 ms. Therefore, the long decay rates of the luminescence are not in contradiction with the hypothesis of porous silicon, on the contrary. We conclude that the high photoluminescence efficiency of porous silicon is not due to a high radiative recombination rate of electron pairs but to a low efficiency of nonradiative processes. As noted in Ref. 22, this originates from the restricted volume available to the carriers.

In Fig. 4, we have reported the calculated radiative recombination rates with respect to the temperature. For clarity, this is done only for some crystallites (results for the others are very similar). The first important point to notice is the quasi-independence of the recombination rate with temperature for $T > 80$ K. Therefore, the large variation of the recombination rate and of the intensity of the luminescence at temperatures above 250 K which has been observed experimentally^{22,46,47} can be only explained by nonradiative or by phonon-mediated radiative recombinations. Of course, the spins of the electron and the hole have been neglected in our calculation and another dependence on temperature is expected because of the singlet ($S = 0$) and triplet ($S = 1$) splitting due to the exchange interaction between particles.^{45,46} This splitting explains well the low-temperature dependence of the luminescence lifetime.^{45,46} But, because this splitting

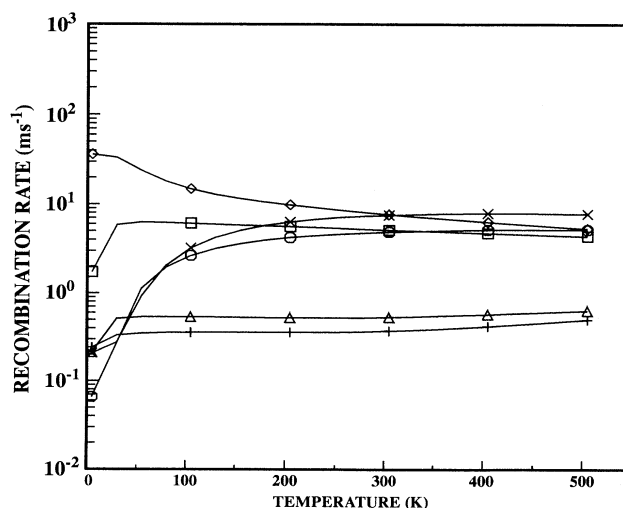


FIG. 4. Dependence of the thermally averaged recombination rates of some typical crystallites on the temperature.

energy is estimated around 10 meV,^{45,46} it must have no effect on the high-temperature dependence of the recombination rate (above 100 K, for example). Therefore, this shows the importance of the nonradiative processes—or here phonon-assisted processes—in the luminescence of porous silicon at high temperature, at least in the model of quantum confinement. Below 80 K, our calculated recombination rates often increase with temperature (a fact that we have verified for many crystallites). As discussed above, this is due to the small valley-orbit splittings between levels with different symmetries ($A_1, E, \text{etc.}$) which are characterized by strongly varying probabilities of optical transitions. Such a temperature dependence is due to the fact that the lowest transition corresponds rarely to the most efficient among all the possible transitions. However, the symmetries of our wave functions are a consequence of the spherical shape of the crystallites. In the case of porous silicon, the crystallites have probably more complex shapes which induce a splitting and a mixing of the various states, maybe averaging the transition probabilities. So we believe that the great diversity in shapes probably reduces a possible variation of the radiative recombination rate at low temperature because of valley-orbit splittings. Anyway, a possible temperature dependence due to valley-orbit interaction cannot be ruled out (a similar conclusion has been obtained recently for silicon wires⁴⁸). The electron-hole exchange interaction is maybe more independent on the crystallite shape and its influence on the low-temperature dependence of radiative recombination rates is probably important as shown in Ref. 45. Finally, in Fig. 5 we give the calculated recombination rates for 110 quantum wires. It is interesting to note that the results are very close to the case of crystallites with no important differences (100 and 111 quantum wires also give similar results). Anyway, we should estimate the influence of the excitonic factor which can be at the origin of an enhancement of the recombination rate.³⁰

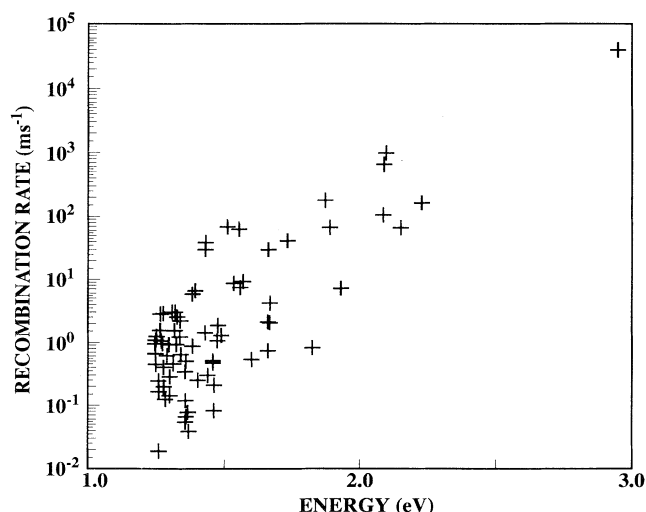


FIG. 5. Same as Fig. 2 but for 110 silicon wires.

IV. OPTICAL ABSORPTION OF SILICON NANOSTRUCTURES

Although most of the studies on porous silicon concern luminescent properties, some of them are related to the optical absorption of this material. Optical absorption is expected to be *a priori* much less sensitive to surface properties.⁴² From comparison between excitation spectra of porous silicon and absorption spectra of silicon molecules, it has been recently deduced that the luminescence of porous silicon could come from silicon molecules.²³ One argument was the sharp absorption edge near ~ 3.2 eV in the excitation spectrum which is much higher than the predicted band gap of crystallites of ~ 3 nm diameter (~ 1.5 eV). However, the threshold of the optical absorption has been measured below 2.0 eV and also shows a blueshift compared to bulk silicon.^{4,42} These shifts can be reasonably related to quantum size effects.⁴² Therefore we have performed a theoretical calculation of the optical absorption of silicon nanostructures in order to see if it is compatible with the experimental results (a calculation of the optical absorption spectrum of quantum wires has been presented in Ref. 17). The optical-absorption coefficient $\alpha(h\nu)$ for a photon energy $h\nu$ is given by

$$\alpha(h\nu) \sim \frac{1}{h\nu} \sum_{n,n'} |\langle n|p|n' \rangle|^2 \delta(E_{n,n'} - h\nu) \quad (3)$$

with notations defined above. We plot in Fig. 6 the optical-absorption coefficient for a small crystallite which is characterized by a calculated band gap of 3.45 eV. We see that the maximum of absorption occurs near 5.0 eV. Anyway, there is a visible peak at 3.45 eV indicating that the absorption near the band edge is already rather efficient. But this kind of crystallite is probably not involved in the luminescence of porous silicon since the ob-

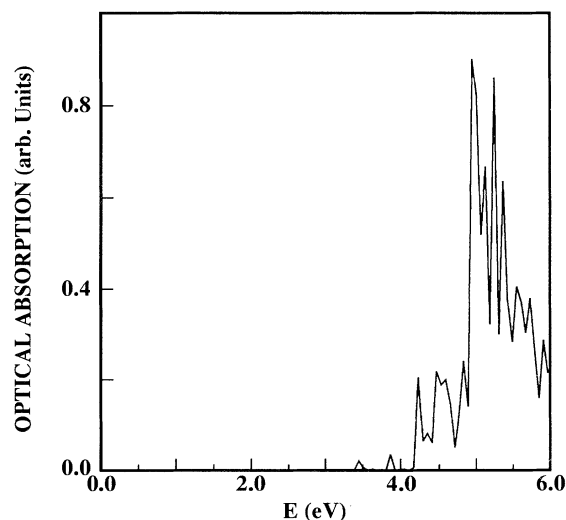


FIG. 6. Optical-absorption coefficient α with respect to the photon energy $h\nu$ calculated for a silicon crystallite with diameter of 1.56 nm. The band gap is calculated at 3.45 eV (without exciton binding energy).

served photon energy is much lower than 3.45 eV.

In Fig. 7 we present the absorption coefficient for a much bigger crystallite with a band gap of 1.67 eV. The absorption edge is shifted near 3.5 eV which corresponds to the direct-gap absorption of bulk silicon. Nothing is visible in the figure between 1.67 and ~ 3.0 eV at that scale. The reason is that the optical matrix element for transitions with energy between 1.67 and 3.0 eV is several orders of magnitude lower than for transitions above 3.0 eV. The optical absorption becomes very close to the one of bulk silicon⁴⁹—but with a blueshift of the absorption edge, i.e., it is very close to the absorption of an indirect semiconductor. Therefore, the excitation spectrum of porous silicon reported in Ref. 23 with an excitation edge above 3.0 eV is compatible with the hypothesis of quantum confinement. In Fig. 8, we plot the absorption coefficient of the same crystallite near the band edge (1.67 eV) but at a different scale and on the form of a bar chart, the amplitudes of the bars representing the integrated absorption coefficient over the width of the bar. In order to compare with the measured optical-absorption spectra reported in Ref. 42, we must take into account the fact that, in the quantum confinement hypothesis, the absorption is the sum of the absorption of numerous crystallites with various shapes and sizes. The main effect of this dispersion could be simply simulated by a broadening of the absorption spectrum of one crystallite. Figure 8 shows that the absorption threshold is at the band-gap energy (1.67 eV) because the transition is dipole allowed even if this is only with fairly weak oscillator strength, compatible with the long radiative lifetime in luminescence. Therefore, the optical threshold is also subject to a blue shift depending on the size of the crystallites in agreement with experiments.^{4,42} It is interesting to note that the absorption coefficient does not follow a linear variation with photon energy but approximately a square

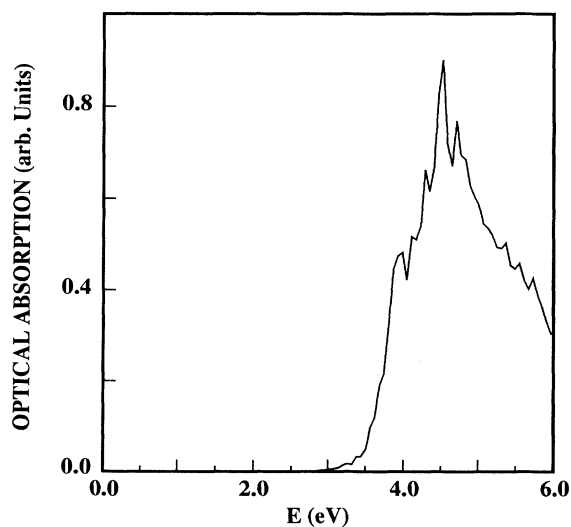


FIG. 7. Optical-absorption coefficient α with respect to the photon energy $h\nu$ calculated for a silicon crystallite with diameter of 3.86 nm. The band gap is calculated at 1.67 eV (without exciton binding energy).

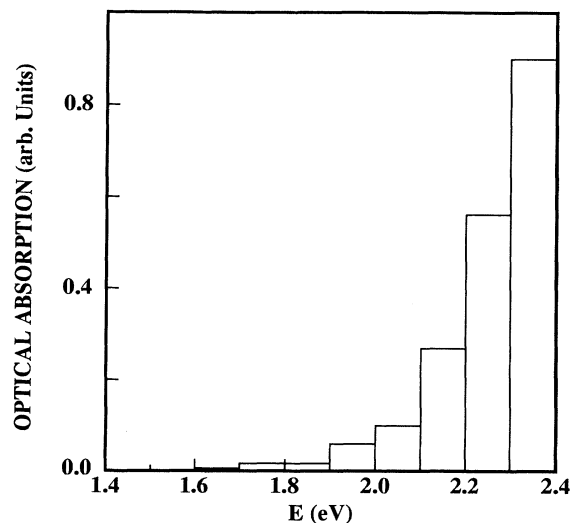


FIG. 8. Optical-absorption coefficient α with respect to the photon energy $h\nu$ calculated for a silicon crystallite with diameter of 3.86 nm. The band gap is calculated at 1.67 eV (without exciton binding energy). Same as Fig. 7 but only the energy region near the band gap is plotted. Amplitudes of the bars represent the integrated absorption coefficient over the width of the bar.

law, in contrast with the experimental absorption spectrum of bulk silicon which is a linear function of photon energy.⁴² Note that the experimental absorption coefficient for *p*-type porous silicon samples (which present the largest blueshift) is also highly nonlinear,³⁵ but it does not follow a power law with photon energy. As discussed in Ref. 42, this may be due to a wide distribution in band-gap energies due to a distribution in sizes and shapes.

V. RECOMBINATION ON DEFECTS IN SILICON CRYSTALLITES

We have seen that nonradiative recombinations are probably more efficient than radiative recombinations at 300 K. We want to discuss now some possible nonradiative mechanisms which can occur in silicon nanostructures. Experimentally, there is some good evidence that hydrogen is present in large quantities in porous silicon in particular at surfaces and that its dissociation strongly decreases the luminescence.^{12,47,50,51} The degradation of the luminescence is correlated with an increase in the density of dangling bonds^{7,52} due, for example, to hydrogen desorption. The adsorption of oxygen induced by light is also a cause for light emission degradation^{51,52,53} but this might be due to the formation of a thin layer of oxide. In effect it is known to introduce many dangling bonds which in this case are not as easily passivated by hydrogen⁵⁴ as during anodic oxidation. Dangling bonds are thus expected to be very efficient nonradiative recombination centers but a quantitative estimation of this influence is needed. The electron-hole recombination on silicon dangling bonds is due to a multiphonon capture of the electron and hole.⁵⁵ Our aim here is to estimate the

probability per unit time that an electron-hole pair created in a silicon crystallite recombines on one dangling bond at the surface of the crystallite. This probability is related to the probabilities W that an electron and a hole in delocalized states are captured in the localized defect state. W is related to the capture coefficient c by $c = \Omega W$ where Ω is the crystal volume⁵⁵ (here, $\Omega = \pi d^3/6$ where d is the crystallite diameter). The validity of the relation $c = \Omega W$ is discussed in the Appendix. A theoretical estimate of c is a difficult task.⁵⁶ However, we can reasonably suppose that the physics of the capture in a crystallite is not very different from the capture in bulk silicon provided that the crystallite is not too small. For example electron paramagnetic resonance experiments show that dangling-bond states in porous silicon are very close to the (111) surface dangling bonds P_b .^{52,57} In bulk silicon, instead of using c , it is common to introduce the capture cross section defined as $\sigma = c/v_{th}$, where v_{th} is the average thermal velocity approximately equal to $v_{th} = \sqrt{8kT/\pi m^*}$ where m^* is the effective mass of the carrier trapped.⁵⁵ One must note here that the concept of capture cross section is quite artificial and the capture coefficient is the meaningful physical quantity.⁵⁵

The situation we want to discuss now corresponds to a crystallite with an electron-hole pair and a neutral dangling bond at the surface. The electron-hole recombination on the dangling bond can be seen as a two step process: first a carrier is captured by the neutral dangling bond and then the second carrier is captured by the charged dangling bond. Cross sections corresponding to the capture of an electron of a hole by a neutral silicon dangling bond at a Si-SiO₂ interface are measured in the 10⁻¹⁴–10⁻¹⁵-cm² range at 170 K.⁵⁶ Cross sections for a capture by a charged dangling bond are not known experimentally. Therefore, we first concentrate on the capture of a carrier on a neutral dangling bond. The capture cross section has a thermally activated behavior which is usually approximated by⁵⁸

$$\sigma \sim \exp \left[-\frac{E_b}{kT} \right] \quad (4)$$

with E_b equal to the barrier height

$$E_b = \frac{(E_0 - d_{FC})^2}{4d_{FC}}, \quad (5)$$

where E_0 is the ionization energy of the defect and d_{FC} is the Franck-Condon shift equal to the energy gain due to lattice relaxation after capture.⁵⁵ d_{FC} is related to the phonon energy $h\nu$ by $d_{FC} = Sh\nu$ where S is the so-called Huang-Rhys factor. It can be shown that Eq. (4) is valid only under restrictive conditions which are fulfilled in the case of the dangling bond in bulk silicon:⁵⁵ strong electron-phonon coupling ($S \gg 1$), high temperature, and $E_0 \sim d_{FC}$. The fact that the Franck-Condon shift is close to the ionization energy in bulk silicon ($E_0 \approx d_{FC}$) explains why the cross section is weakly thermally activated.⁵⁶ This situation is summarized on the configuration

coordinate diagram of Fig. 9 which is valid both for the capture of a hole or an electron by a dangling bond (energies are very similar for the two processes⁵⁶).

Because of the quantum confinement, the ionization energy E_0 in crystallites is different from its bulk silicon value. The dangling-bond state is fairly localized and its energy will remain constant on an absolute energy scale when the confinement is varied. Thus the change ΔE in the ionization energy E_0 is due to the shift of the band edges. We have seen above that the shift is not the same for the hole and for the electron but the difference remains small. For example, it is close to 0.3–0.4 eV (for the hole and for the electron) for a blueshift of 0.7 eV. On the contrary, the Franck-Condon shift is unaffected by the confinement because it only depends on the local atomic relaxation (Fig. 9).

From Eq. (4) we expect a strong decrease of the cross section with the ionization energy and, therefore, with confinement. But to estimate this change, Eq. (4) is no longer valid because the condition $E_0 \approx d_{FC}$ is not verified any more when ΔE is important. We are also interested in the dependence of the cross section over a wide range of temperatures for which Eq. (4) is not accurate enough. To improve on this, we make use of a recently proposed analytic expression of the capture coefficient which remains valid over the whole temperature range, any ionization energy, and any strength of the coupling between the lattice and the defect.⁵⁵ The capture coefficient c is written as $c_0 R$ where c_0 is a coefficient whose dependence on T and E_0 is weak and R is a dimensionless function in which the dependence on the same parameters is important. R is given by^{55,59}

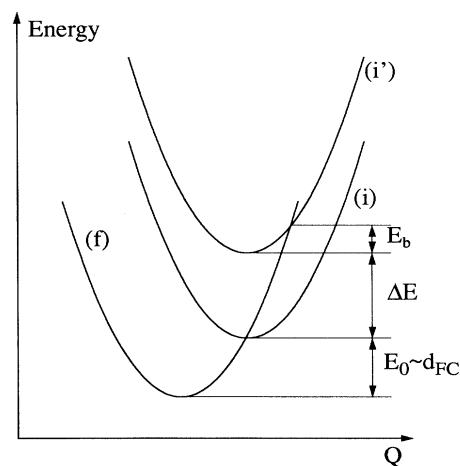


FIG. 9. Configuration coordinate diagram, representing the variation of the total energy versus the atomic displacement for two charge states of the defect [initial (i) and final (f)]. Two initial states are indicated, one (i) in bulk silicon (ionization energy E_0) and the other (i') in a silicon crystallite (ionization energy $E_0 + \Delta E$). The situation in bulk silicon corresponds to a negligible barrier for the capture. In silicon crystallites, the increase in ionization energy creates a barrier E_b for the recombination (in a classical picture).

$$R = \frac{1}{\sqrt{2\pi}} \left[\left(\frac{E_0}{h\nu} \right)^2 + z^2 \right]^{-1/4} \exp \left\{ -S \coth \left[\frac{h\nu}{2kT} \right] + \frac{E_0}{2kT} + \left[\left(\frac{E_0}{h\nu} \right)^2 + z^2 \right]^{1/2} - \frac{E_0}{h\nu} \sinh^{-1} \left[\frac{E_0}{h\nu z} \right] \right\},$$

with $z = \frac{S}{\sinh \left[\frac{h\nu}{2kT} \right]}$. (6)

In Fig. 10 we plot the capture cross section of a single dangling bond with respect to the shift ΔE in the ionization energy E_0 . We take the cross section equal to 10^{-15} cm² at 170 K which is a lower limit of the measured values.⁵⁶ This is valid for captures of electrons and holes because the measured values are quite close for the two processes at the neutral center. We also take $h\nu=20$ meV and $S=15$.⁵⁶ The dependence of σ on the ionization energy is very strong, over several decades. In the approximate classical terms of Eq. (4), this is due to the increase of the energy barrier for carrier capture with ionization energy. Figure 10 shows that the dependence of σ on temperature is weak when the shift in ionization energy is small because the energy barrier is negligible. But when the ionization energy increases, the dependence becomes important as expected. Finally, we must add that the dependence of σ on temperature and on ionization energy might be observed by measurements of the kinetics of capture of excited carriers using optical or electrical experiments. This would be a very good proof of the quantum confinement hypothesis.

Now we can come to the main aim of this section, which is the comparison of the nonradiative capture due to a single dangling bond in a crystallite with the intrinsic radiative recombination. We estimate the nonradiative capture rate W using the previous formulas. It depends on the size of the crystallites through Ω and on the ion-

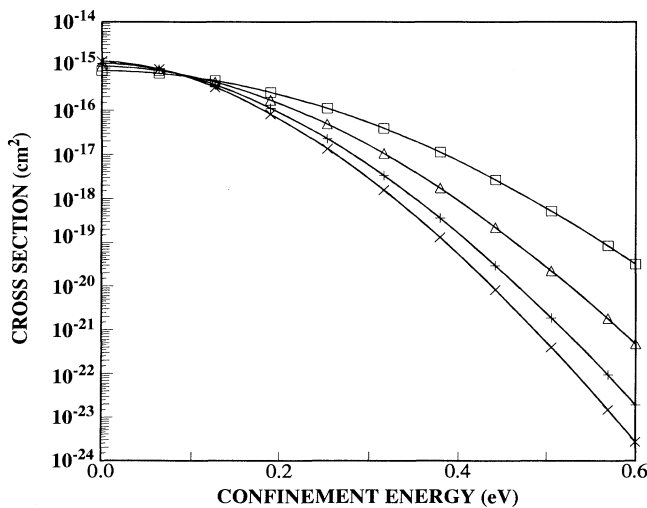


FIG. 10. Dependence of the capture cross section σ of an isolated dangling bond with respect to the increase ΔE in the ionization energy E_0 due to confinement (for holes or electrons) at $T=300$ K (\square), $T=170$ K (\triangle), $T=100$ K ($+$), and $T=20$ K (\times).

ization energy through σ (which itself depends on the size). In Figs. 11 and 12 we plot W with respect to the electron-hole energy in the crystallites, respectively, at $T=5$ K and 300 K. For comparison, we also show the calculated radiative recombination rates (same as Figs. 2 and 3). W decreases at high energy because of the increase in the barrier. It decreases faster at $T=5$ than at 300 K because the process is strongly thermally activated when the energy barrier becomes important. At energies close to the bulk band gap, W also decreases very quickly because the volume of the corresponding crystallite tends to infinity and the probability to be captured by a single dangling bond vanishes. For photon energies in the range of interest for the visible luminescence of porous silicon (1.4–2.2 eV), the nonradiative capture is much faster than the radiative recombination, particularly at $T=300$ K. We deduce that the presence of one silicon dangling bond at the surface of a crystallite in porous silicon kills its luminescence above 1.1 eV, in agreement with experiments.^{7,52} But Figs. 11 and 12 show that for small crystallites the nonradiative capture on a silicon dangling bond becomes less efficient than the intrinsic radiative recombination (for a photon energy higher than 2.2 and 2.6 eV, respectively, at $T=5$ and 300 K). This may be of interest for the optical properties of small sil-

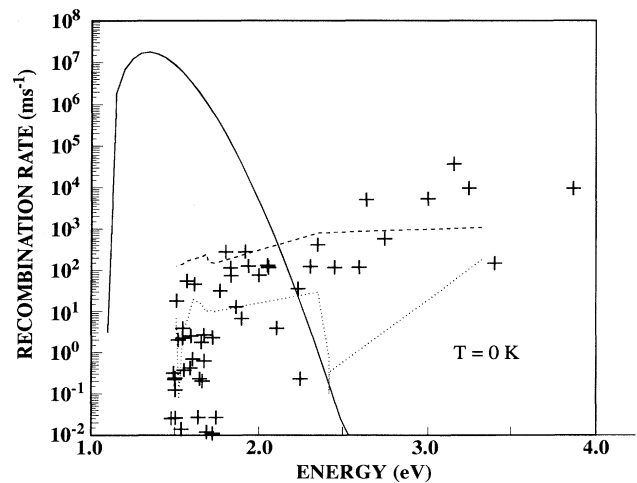


FIG. 11. Capture rates ($T=5$ K) of an electron or a hole in silicon crystallites due to a nonradiative capture on a single neutral silicon dangling bond plotted with respect to the excitonic band-gap energy of the crystallites (continuous line). Crosses give the radiative recombination rates of the electron-hole pairs in the same crystallites. The other curves are the radiative capture rates of carriers on a neutral dangling bond (hole capture: — — —; electron capture:).

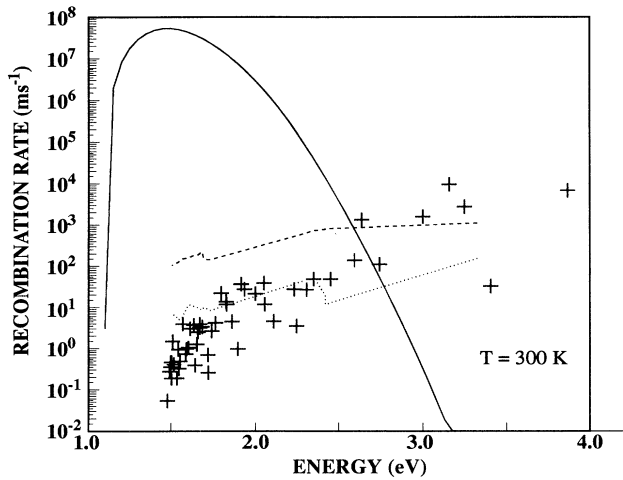


FIG. 12. Capture rates ($T=300$ K) of an electron or a hole in silicon crystallites due to a nonradiative capture on a single neutral silicon dangling bond plotted with respect to the excitonic band-gap energy of the crystallites (—). Crosses give the radiative recombination rates of the electron-hole pairs in the same crystallites. The other curves are the radiative capture rates of carriers on a neutral dangling bond (hole capture: — —; electron capture:).

icon nanostructures.

In bulk silicon, the recombination on a silicon dangling bond is mostly a nonradiative process. This means that the radiative capture of carriers on a dangling bond is inefficient compared to the multiphonon capture. In small silicon crystallites, we have just seen that the nonradiative capture efficiency strongly decreases compared to bulk silicon. Therefore, we can expect that the radiative capture on a silicon dangling bond becomes comparable to other processes in crystallites. We have calculated the radiative capture rate of an electron and a hole by a single neutral dangling bond in the silicon crystallites previously investigated. We first calculate the electronic structure of the crystallites with one silicon dangling bond at the surface. This is simply done by removing one hydrogen atom of the crystallite. The radiative capture rates are calculated by using Eqs. (1) and (2). Results are plotted in Figs. 11 and 12 (hole capture: dashed line; electron capture: dotted line). The oscillations in the curves have the same origin than the dispersion of the intrinsic radiative recombination rates that we have previously described. They only appear at very low temperature (Fig. 11). We see that in average the radiative capture time is between 1 and 10 μs for the capture of a hole and between 10 and 100 μs for the capture of an electron. Therefore, for crystallites with an optical band gap lower than 2.2 eV, the nonradiative capture is much faster than the radiative capture. For crystallites with a higher optical band gap, the situation can be inverted depending on the temperature. In that case, we see in Figs. 11 and 12 that the intrinsic radiative recombination and the radiative capture are with comparable efficiency.

From the above discussion, we show that for crystallites with an optical band gap of lower than 2.2 eV the

presence of a neutral dangling bond leads to the nonradiative capture of the electron or the hole (more probably the electron because the confinement energy is slightly lower for the electron than for the hole and therefore the capture barrier is smaller). So, in any case, a carrier remains in the conduction band or the valence band. We can now discuss its capture by the charged dangling bond. The situation is summarized on the configuration coordinate diagram of Fig. 13. The lower energy curve corresponds to the ground state of the crystallite with one neutral dangling bond at the surface. The higher curve describes the system after optical excitation of an electron in the conduction band. The intermediate curve is the total energy after capture of the first carrier on the dangling bond. These two higher curves are equivalent to those labeled (*i'*) and (*f*) in Fig. 9. The vertical shift ΔE is the confinement energy. It is equal to the confinement energy ΔE_c of the conduction band with respect to the bulk silicon conduction band in the case where the first particle to be captured is an electron. It is equal to ΔE_v in the case of the capture of the hole. E_{b1} is the energy barrier (in a classical point of view) for this capture of the first carrier which has been analyzed above. E_{b2} is the energy barrier for the multiphonon cap-

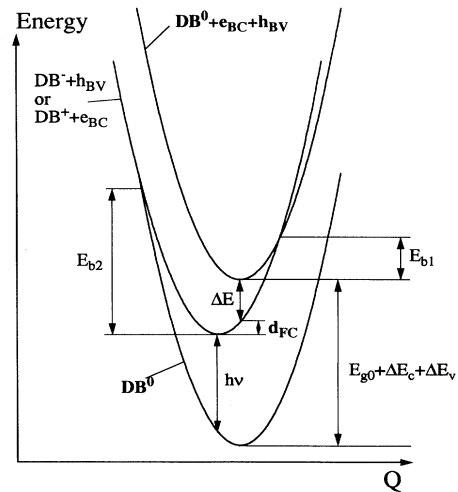


FIG. 13. Configuration coordinate diagram, representing the variation of the total energy of a crystallite with one dangling bond at the surface. The ground state (lower curve) corresponds to filled valence states, empty conduction states, and the dangling bond in the neutral charge state (DB^0). The higher curve [equivalent to curve (*i'*) of Fig. 9] represents the same system after excitation of an electron in the conduction band leaving a hole in the valence band ($\text{DB}^0 + e_{\text{BC}} + h_{\text{BV}}$). The intermediate curve [equivalent to curve (*f*) of Fig. 9; the curve (*i*) of Fig. 9 is not reproduced here] describes the system after capture of a carrier by the dangling bond. Two situations are possible: the capture of the electron, the hole remaining in the valence band ($\text{DB}^- + h_{\text{BV}}$) or the capture of the hole, the electron remaining in the conduction band ($\text{DB}^+ + e_{\text{BC}}$). ΔE is the energy shift of the conduction or the valence band due to confinement compared to the bulk silicon band structure (conduction for the capture of the electron, valence for the capture of the hole).

ture of the second carrier which we want to discuss now. Compared to the first capture, the second one involves much larger energies (the sum of the thermal ionization energies is equal to the bandgap energy). From Fig. 13 and Eq. (5), we can calculate the energy barrier E_{b2} . We obtain

$$E_{b2} = \frac{(E_{g0} + \Delta E - 2d_{FC})^2}{4d_{FC}}, \quad (7)$$

where E_{g0} is the bulk silicon band-gap energy and ΔE is the confinement energy of the band corresponding to the carrier involved in the second capture (ΔE_c for the electron, ΔE_v for the hole). For a confinement energy ΔE of 0.3 eV, E_{b2} is equal to 0.53 eV which is a very large barrier for a multiphonon capture. Therefore, the capture cross section for the second capture should be strongly reduced compared to the first one [injecting the appropriate values in (6) gives a reduction factor of 3×10^{-7} at $T = 300$ K and 5×10^{-11} at $T = 10$ K]. But this does not take into account the fact that the dangling bond is charged and that the capture must be enhanced by the Coulomb interaction. The numerical estimation of this enhancement is difficult task and will not be done here. Anyway, due to the large barrier E_{b2} , we can conclude that the second capture may become a radiative process, at least at low temperature. The energy of the emitted photon ($h\nu$ in Fig. 13) should be equal to $E_{g0} + \Delta E - 2d_{FC}$ which is about 0.8 eV for a ΔE of 0.3 eV. Note that an infrared emission from porous silicon has been reported recently and interpreted as due to the radiative recombination on silicon dangling bonds.⁶¹ Our study concludes that this interpretation is coherent with the hypothesis of quantum confinement and that the photon emission would correspond to the capture of the second carrier, more probably the hole.

From comparison of Figs. 12 and 3 we see that the nonradiative recombination rate on a silicon dangling bond is several orders of magnitude higher than the experimental decay time of the luminescence at $T = 300$ K. Therefore, the presence of silicon dangling bonds in the crystallites cannot explain the decay time of the luminescence. Other nonradiative processes must be involved. In bulk silicon, the Auger effect is an important mechanism of nonradiative recombination.⁶⁰ This process involves three particles, one electron and two holes or two electrons and one hole. So it requires an extra electron or hole with the excited electron-hole pair. In the hypothesis of quantum confinement in silicon crystallites, the probability to find an impurity or a defect is low due to the small number of atoms in the crystallite ($< 10^5$).²² Therefore, the probability to have an extra hole or electron due to the doping is weak and the Auger effect should be ruled out. This is one additional argument explaining the long decay time of the luminescence. Note that this conclusions is not valid in the case of infinite silicon wires. Another possible process for nonradiative deexcitation is the tunneling of carriers through oxide barriers surrounding the confined zone. It seems to explain quite well the experimental results.²²

VI. CONCLUSION

We have shown that the luminescence of porous silicon can be explained by quantum confinement of the electron-hole pairs in quantum crystallites or wires with diameters lower than 4.5 nm. The confinement induces band mixing which gives dipole allowed band-gap transitions but we show that the optical matrix elements remain small. The calculated radiative recombination rate is lower than the experimental decay time of the luminescence, meaning that nonradiative recombination is probably involved. We have also found that the optical absorption of silicon crystallites is very close to the one of bulk silicon with a sharp edge above 3.0 eV. The low temperature dependence of the radiative decay time of the luminescence could be explained by the exchange splitting in the lowest exciton state but the influence of the valley-orbit splitting is not excluded. We have also studied the nonradiative capture of carriers on silicon dangling bonds in silicon crystallites. We demonstrate that the capture is very dependent on the confinement energy because of the apparition of a barrier for the capture. Anyway the presence of one silicon dangling bond in a crystallite of porous silicon must destroy its luminescence in the 1.4–2.2 eV range. For small crystallites which can emit photons with energy higher than 2.2 eV, we have shown that the nonradiative recombination on dangling bonds becomes less efficient than the radiative recombination. The recombination of electron-hole pairs on a dangling bond in a crystallite may be at the origin of the luminescence in the infrared region.

ACKNOWLEDGMENT

Institut d' Electronique et de Microelectronique du Nord is UMR No. 9929 of CNRS.

APPENDIX: VOLUME DEPENDENCE OF THE PROBABILITY OF CAPTURE

To calculate the probability W of nonradiative capture of a carrier by a single dangling bond, we have used the relation $W = c/\Omega$ where c is the capture coefficient and Ω is the crystal volume. If we forget the dependence of the capture coefficient itself on the crystallite size—due to the dependence on the crystallite band gap as discussed in Sec. V—this relation naturally means that the probability of capture W is inversely proportional to the crystallite volume Ω . The reason is that this probability is somehow proportional to the overlap between the extended wave function of the carrier and the localized wave function of the defect which, for bulk states, exactly scales as $1/\Omega$. However, it is not clear if this is still valid in the case of a surface—or interface—defect where the wave function of the carrier has a sharp variation on a small distance in the vicinity of the defect. The aim of the appendix is to discuss the volume dependence of the probability of capture by a surface or interface defect.

In Fig. 14, we show a simplified representation of a Si-SiO₂ interface which is of interest here for the P_b center. The transition between the Si and SiO₂ is not abrupt, there is a zone with intermediate composition SiO_x. The

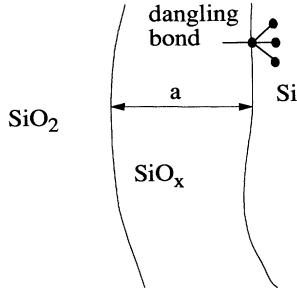


FIG. 14. Representation of a Si-SiO₂ interface with an intermediate zone of approximate composition SiO_x. The width of this region is denoted by a .

width a of this intermediate region is of the order of 5 Å. Let us assume that the defect, the dangling bond, is localized at the Si-SiO_x interface (note that this assumption has no incidence on the conclusions of the appendix and that the following discussion still holds in the case of a surface or of another interface). Because of the large SiO₂ band gap, the wave function of the carriers tends to zero at the SiO₂-SiO_x interface which we take as the origin of the positions. As already mentioned, the probability of capture W is proportional to a matrix element $|\langle \psi_{\text{loc}} | V | \psi_k \rangle|^2$ where $|\psi_{\text{loc}}\rangle$ is the localized defect wave function and $|\psi_k\rangle$ is the wave function of the free carrier. Let us discuss this term in two cases of interest, for a semi-infinite system and for a spherical crystallite.

The first case we want to discuss corresponds to a planar Si-SiO_x-SiO₂ interface with a semi-infinite Si bulk material (x being the growth direction). The wave functions of the free carriers in the bulk correspond to Bloch functions. Because the boundary conditions impose that they vanish at $x=0$, the wave functions (in a simple envelope function treatment) can be written as

$$\frac{\sin(kx)}{\sqrt{L}} \frac{e^{ik_{\parallel}r_{\parallel}}}{\sqrt{S}}$$

where the normalization has been made over a volume $\Omega=LS$, k is the projection of the momentum in the x direction, and k_{\parallel} and r_{\parallel} are, respectively, the projections of the momentum and the particle vector position in the (y,z) plane. Then the probability of capture is proportional to

$$W \propto \left| \int \frac{\sin(kx)}{\sqrt{L}} \frac{e^{ik_{\parallel}r_{\parallel}}}{\sqrt{S}} V_{\text{loc}} dx dr_{\parallel} \right|^2 \propto \frac{\sin(ka)^2}{\Omega}, \quad (\text{A1})$$

where the integration is made over the defect volume situated at $x \sim a$. As the system is macroscopic, the k states form a band and one must take the thermal average of the probability (A1). This results in the replacement of $\sin(ka)^2$ by $\int \sin(ka)^2 f(k,T) dk$, where $f(k,T) dk$ is the probability of occupancy of the state k at temperature T . Therefore, there is no longer a dependence of the probability on k in Eq. (A1) and the probability is simply proportional to $1/\Omega$. We deduce that the probability of capture of carriers by surface or interface defects follows the same volume dependence than in the case of bulk defects

if the system is macroscopic. This is confirmed by many experimental results. For example, the decay rate of the electron-hole pairs at the Si or Ge surfaces follows a $1/L$ law where L is the thickness of the sample.⁶⁰

The second case we discuss corresponds to a spherical crystallite of silicon embedded in a SiO₂ matrix. The representation of Fig. 14 still holds but with curved interfaces. The wave function of the carriers is of the form $\sin(kr)/\sqrt{Rr}$ where r has its origin at the center of the crystallite and R is the radius of the sphere described by the SiO₂-SiO_x interface. Since the wave function vanishes at $r=R$, k is equal to π/R for the ground state. The probability of capture is given by

$$W \propto \left| \int \frac{\sin(kr)}{\sqrt{Rr}} V_{\text{loc}} d^3r \right|^2 \propto \frac{\sin[k(R-a)]^2}{R^3} = \frac{\sin(ka)^2}{R^3}. \quad (\text{A2})$$

We see that the form of Eq. (A2) is quite comparable to the one of Eq. (A1) in the case of a semi-infinite system. Note that when the size of the crystallite increases ("macroscopic limit") one would find the same behavior in the two cases and the thermal averaging would give the same $(1/R^3) \propto (1/\Omega)$ dependence. But the interesting case corresponds to small crystallites where the energy splitting between the ground state and the first excited state of the crystallite is larger than the thermal energy kT . In that case, only the ground state corresponding to $k=\pi/R$ is populated. Then, as the dimensions of the crystallite are still large compared to a , $ka=\pi(a/R) \ll 1$ and the probability of capture becomes proportional to $1/R^5$. Therefore the simple rule $W=c/\Omega$ is no longer valid in the case of the capture of defects at the surface of small crystallites. In Fig. 15, we have drawn the dependence of W with respect to the radius R of the crystallite (it only takes into account the dependence due to the

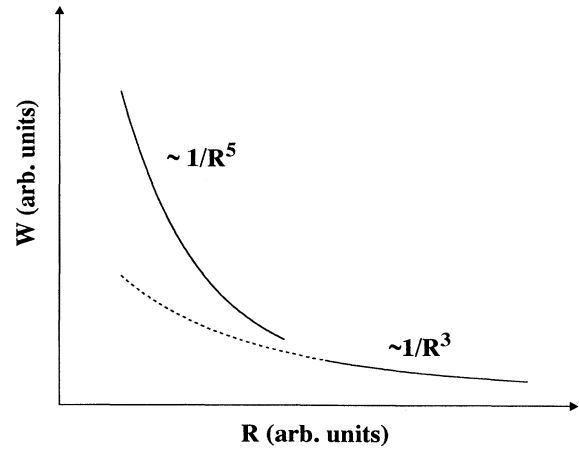


FIG. 15. Variation of the capture probability W of a carrier by a dangling bond at surface of a crystallite as function of the radius of the crystallite R due to the variation of the overlap between the wave function of the carrier and the wave function of the defect (other sources of variation are not included).

variation of the overlap between the carrier and defect wave functions). At large R , i.e., when the spacing between confined states is small compared to the thermal energy kT , it behaves as $1/R^3$. For smaller R , it behaves as $1/R^5$.

From the above conclusions, the validity of the results presented throughout this paper concerning the nonradiative capture on a dangling bond at surface of a crystallite could be questioned. To do this calculation, we have used the relation $W=c/\Omega$, the capture coefficient c being deduced from its experimental value for the P_b center at Si-SiO₂ interface (which is equivalent to the semi-infinite system described above). We have seen that this procedure is perfectly valid in the case of big crystallites. However, in the case of interest here, a correction must be included to account for a different variation of the

overlap of the wave functions with respect to the crystallite radius. As seen in Fig. 15, taking a simple $1/R^3$ law, we have underestimated the probability W (the calculated value would correspond to the continuation of the $1/R^3$ law at low radius represented by a dashed line in Fig. 15). Therefore, the conclusion that the presence of dangling bond in a silicon crystallite destroys its visible luminescence is still strengthened by this correction. To estimate numerically the amplitude of the correction is not simple. Anyway, we have already seen that the dependence of the capture coefficient on the size of the crystallite involves changes of several orders of magnitude and, obviously, this conclusion will not be significantly altered by such a correction. In the same spirit, the conclusion that the capture of a carrier by a charged dangling bond must be a radiative process will not change.

-
- ¹L. T. Canham, *Appl. Phys. Lett.* **57**, 1046 (1990).
- ²A. Halimaoui, C. Oules, G. Bomchil, A. Bsiesy, F. Gaspard, R. Herino, M. Ligeon, and F. Muller, *Appl. Phys. Lett.* **59**, 304 (1991).
- ³A. Bsiesy, J. C. Vial, F. Gaspard, R. Hérino, M. Ligeon, F. Muller, R. Romestain, A. Wasiela, A. Maimaoui, and G. Bomchil, *Surf. Sci.* **254**, 195 (1991).
- ⁴V. Lehmann and U. Gosele, *Appl. Phys. Lett.* **58**, 856 (1991).
- ⁵M. S. Brandt, H. D. Fuchs, M. Stutzmann, J. Weber, and M. Cardona, *Solid State Commun.* **81**, 307 (1992).
- ⁶S. M. Prokes, *J. Appl. Phys.* **73**, 407 (1992).
- ⁷S. M. Prokes, W. E. Carlos, and V. M. Bermudez, *Appl. Phys. Lett.* **61**, 1447 (1992).
- ⁸R. W. Fathauer, T. George, A. Ksendzov, and R. P. Vasquez, *Appl. Phys. Lett.* **60**, 995 (1992).
- ⁹N. Noguchi, I. Suemune, M. Yamanishi, G. C. Hua, and N. Otsuka, *Jpn. J. Appl. Phys.* **31**, 229 (1992).
- ¹⁰T. Ito, T. Ohta, and A. Hiraki, *Jpn. J. Appl. Phys.* **31**, L1 (1992).
- ¹¹S. Shih, C. Tsai, K.-H. Li, K. H. Jung, J. C. Campbell, and D. L. Kwong, *Appl. Phys. Lett.* **60**, 633 (1992).
- ¹²Y. H. Xie, W. L. Wilson, F. M. Ross, J. A. Mucha, E. A. Fitzgerald, J. M. Macaulay, and T. D. Harris, *J. Appl. Phys.* **71**, 2403 (1992).
- ¹³Z. Sui, P. P. Leong, I. P. Herman, G. S. Higashi, and H. Temkin, *Appl. Phys. Lett.* **60**, 2086 (1992).
- ¹⁴M. W. Cole, J. F. Harvey, R. A. Lux, D. W. Eckart, and R. Tsu, *Appl. Phys. Lett.* **60**, 2800 (1992).
- ¹⁵F. Kozlowski, and W. Lang, *J. Appl. Phys.* **72**, 5401 (1992).
- ¹⁶M. Voos, Ph. Uzan, C. Delalande, G. Bastard, and A. Halimaoui, *Appl. Phys. Lett.* **61**, 1213 (1992).
- ¹⁷G. D. Sanders and Y. Chang, *Phys. Rev. B* **45**, 9202 (1992).
- ¹⁸T. Ohno, K. Shiraiishi, and T. Ogawa, *Phys. Rev. Lett.* **69**, 2400 (1992).
- ¹⁹J. P. Proot, C. Delerue, and G. Allan, *Appl. Phys. Lett.* **61**, 1948 (1992).
- ²⁰S. Y. Ren and J. D. Dow, *Phys. Rev. B* **45**, 6492 (1992).
- ²¹E. F. Steigmeier, B. Delley, and H. Auderset, *Phys. Scr. T* **45**, 305 (1992).
- ²²J. C. Vial, A. Bsiesy, F. Gaspard, R. Hérino, M. Ligeon, F. Muller, R. Romestain, and R. M. Macfarlane, *Phys. Rev. B* **45**, 14 171 (1992).
- ²³Y. Kanemitsu, K. Suzuki, H. Uto, Y. Masumoto, T. Matsumoto, S. Kyushin, K. Higushi, and H. Matsumoto, *Appl. Phys. Lett.* **61**, 2446 (1992).
- ²⁴A. G. Cullis and L. T. Canham, *Nature* **353**, 335 (1991).
- ²⁵R. Tsu, H. Shen, and M. Dutta, *Appl. Phys. Lett.* **60**, 112 (1992).
- ²⁶T. George, M. S. Anderson, W. T. Pike, T. L. Lin, R. W. Fathauer, K. H. Jung, and D. L. Kwong, *Appl. Phys. Lett.* **60**, 2359 (1992).
- ²⁷V. Vezin, P. Goudeau, A. Naudon, A. Halimaoui, and G. Bomchil, *Appl. Phys. Lett.* **60**, 2625 (1992).
- ²⁸D. Bellet, G. Dolino, M. Ligeon, P. Blanc, and M. Krisch, *J. Appl. Phys.* **71**, 145 (1992).
- ²⁹P. B. Allen, J. Q. Broughton, and A. K. McMahan, *Phys. Rev. B* **34**, 859 (1986).
- ³⁰A. J. Read, R. J. Needs, K. J. Nash, L. T. Canham, P. D. J. Calcott, and A. Qteish, *Phys. Rev. Lett.* **69**, 1232 (1992); **70**, 2050 (E) (1993).
- ³¹F. Buda, J. Kohanoff, and M. Parrinello, *Phys. Rev. Lett.* **69**, 1272 (1992).
- ³²T. Takagahara and K. Takeda, *Phys. Rev. B* **46**, 15 578 (1992).
- ³³F. Huaxiang, Y. Ling, and X. Xide, *J. Phys. Condens. Matter* **5**, 1221 (1993).
- ³⁴M. V. RamaKrishna and R. A. Friesner, *J. Chem. Phys.* **96**, 873 (1992).
- ³⁵J. Chelikowsky and J. Phillips, *Phys. Rev. Lett.* **63**, 1653 (1989).
- ³⁶Y. Kayanuma, *Solid State Commun.* **59**, 405 (1986); *Phys. Rev. B* **38**, 9797 (1988).
- ³⁷S. Furukawa and T. Miyasato, *Phys. Rev. B* **38**, 5726 (1988).
- ³⁸M. S. Hybertsen, in *Light Emission from Silicon*, edited by S. S. Iyer, L. T. Canham, and R. T. Collins, MRS Proceedings No. 256 (Material Research Society, Pittsburgh, 1992), pp. 179–184.
- ³⁹Some results on the radiative recombination rates were already published in a previous paper (Ref. 19), but some small differences exist with the present paper. Reference 19 concerned a smaller number of crystallites than here. The calculation was done without taking the temperature into account and some degeneracies was not correctly included. In addition, we did not know at this time a realistic value for the refraction index n of porous silicon and we used $n=2.6$. Here we have used $n=1.33$.
- ⁴⁰D. L. Dexter, in *Solid State Physics, Advances in Research and*

- Applications*, edited by F. Seitz and D. Turnbull (Academic, New York, 1958), Vol. 6, p. 360.
- ⁴¹C. Pickering, M. I. J. Beale, D. J. Robbins, P. J. Pearson, and R. Greef, *Thin Solid Films* **125**, 157 (1985).
- ⁴²I. Sagnes, A. Halimaoui, G. Vincent, and P. A. Badoz, *Appl. Phys. Lett.* **62**, 1155 (1993).
- ⁴³J. Petit, G. Allan, and M. Lannoo, *Phys. Rev. B* **33**, 8595 (1986).
- ⁴⁴J. Petit, M. Lannoo, and G. Allan, *Solid State Commun.* **60**, 861 (1986).
- ⁴⁵P. D. J. Calcott, K. J. Nash, L. T. Canham, M. J. Kane, and D. Brumhead, *J. Phys. Condens. Matter* **5**, L91 (1993).
- ⁴⁶J. C. Vial, A. Bsiesy, G. Fishman, F. Gaspard, R. Hérino, M. Ligeon, F. Muller, R. Romestain, and R. M. Macfarlane, in *Microcrystalline Semiconductors, Material Science and Device*, edited by Y. Aoyagi, L. T. Canham, P. Fauchet, I. Shimizu, and C. C. Tsai, MRS Symposia Proceedings No. 283 (Material Research Society, Pittsburgh, 1993), p. 241.
- ⁴⁷C. Tsai, K.-H. Li, J. Sarathy, S. Shih, J. C. Campbell, B. K. Hance, and J. M. White, *Appl. Phys. Lett.* **59**, 2814 (1991).
- ⁴⁸M. S. Hybertsen and M. Needels, *Phys. Rev. B* **48**, 4608 (1993).
- ⁴⁹*Semiconductors, Group IV Elements and III-V Compounds*, edited by O. Madelung (Springer-Verlag, New York, 1991).
- ⁵⁰R. T. Collins, M. A. Tischler, and J. H. Stathis, *Appl. Phys.* **61**, 1649 (1992).
- ⁵¹M. B. Robinson, A. C. Dillon, D. R. Haynes, and S. M. George, *Appl. Phys. Lett.* **61**, 1414 (1992).
- ⁵²M. S. Brandt and M. Stutzmann, *Appl. Phys. Lett.* **61**, 2569 (1992).
- ⁵³Z. Y. Xu, M. Gal, and M. Gross, *Appl. Phys. Lett.* **60**, 1375 (1992).
- ⁵⁴I. H. Poindexter and P. J. Caplan, *Prog. Surf. Sci.* **14**, 201 (1983).
- ⁵⁵D. Goguenheim and M. Lannoo, *J. Appl. Phys.* **68**, 1059 (1990).
- ⁵⁶D. Goguenheim and M. Lannoo, *Phys. Rev. B* **44**, 1724 (1991).
- ⁵⁷H. J. von Bardeleben, D. Stievenard, A. Grosman, C. Ortega, and J. Siejka, *Phys. Rev. B* **47**, 10 899 (1993).
- ⁵⁸C. H. Henry and D. V. Lang, *Phys. Rev. B* **15**, 989 (1977).
- ⁵⁹There is a misprint in the last term of Eq. (29) of Ref. 55. The right equation is the Eq. (6) of the present paper.
- ⁶⁰E. Yablonovitch, D. L. Allara, C. C. Chang, T. Gmitter, and T. B. Bright, *Phys. Rev. Lett.* **57**, 249 (1986).
- ⁶¹B. K. Meyer, D. M. Hofmann, W. Stadler, V. Petrova-Koch, F. Koch, P. Omling, and P. Emanuelsson (unpublished).